COMPUTERS AND INFORMATICS
2757-8259 2024, Volume 4 Issue 2
DOI: 10.62189/ci.1267901 Research Article

Pansharpening through orthogonal projection of data

Mutum Bidyarani Devi*
Manipur International University, Department of Electronics and Computer Sciences, Imphal, India,
bidyarani.mutum@gmail.com
Rajagopalan Devanathan
Hindustan Institute of Technology and Science, Department of Electrical and Electronics Engineering, Chennai, India,
pt.devanathanr@hindustamuniv.ac.in

Submitted: *20.03.2023*
Accepted: *05.02.2024*
Published: *01.12.2024*

* *Corresponding Author*

Abstract:

With the increase in the amount of satellite data particularly in the form of satellite images, the need to fuse heterogeneous imagery has become an important research area. Pansharpening is an image fusion method that involves fusing a high spatial resolution panchromatic imagery and a high spectral resolution multispectral imagery to obtain an image that possesses spatial and spectral data both in high resolution. In this paper, a pansharpening method based on a classical information-theoretic result of orthogonal projection between two sets of correlated data is proposed. The originality of the study lies in the application of the information-theoretic approach to pansharpening which has not been reported to date. The proposed method which is illustrated using IKONOS data is also compared favorably with existing pansharpening methods such as IHS, Brovey, PCA, SFIM, HPF, and Multi methods using standard evaluation criteria, such as Chi-square test (X^2), R2 test, RMSE, SNR, spectral discrepancy (SD) and ERGAS.

Keywords: *Data fusion, IKONOS, Image fusion, Information correlation, Pansharpening*

Cite this paper as: Devi, M.B., & Devanathan, R., Pansharpening through the orthogonal projection of data, *Computers and Informatics*, 2024; 4(2); 51-64, https://doi.org/10.62189/ci.1267901

1. INTRODUCTION

Image fusion is a process of integrating two complementary signals to produce a composite output that is different from the original signals. Image fusion is used for accurate targeting, accurate classification, image enhancement, and so forth. There are numerous applications of image fusion in various fields – military surveillance, medical imaging, and many more. The more recent application of image fusion has been reported in the geospatial fields. In the last few decades, geospatial technology has taken a new dimension with the successful launching of earth observation satellites. Concurrently, advancements in computing technology and data science have enabled the storage and analysis of satellite data in a meaningful way. Particularly, there have been recent developments in the area of remote sensing. Remote sensing has been successfully applied in agriculture, forestry, urbanization, photogrammetry, hydrology, geology, and so forth.

With the availability of remotely sensed satellite imagery for public use, there has been a tremendous increase in the utilization of the data for various applications. Some of the sensors onboard the satellite provide images of different resolutions. Some of the sensors provide a single type of image while other sensors provide different types of images simultaneously. The importance of image fusion in remote sensing arises when there is a need for high-quality images for a particular application. Since the sensor provides either a high spatial resolution image associated with low spectral resolution or a high spectral resolution image but with low spatial resolution, a single image may not be enough to fulfill the requirements of a given application.

The single-color channel or monochrome imagery is sometimes called panchromatic imagery while the multicolor or multichannel imagery is called multispectral imagery. Panchromatic image has spatially high resolution but the multispectral imagery has spatially low resolution. Often these two imageries are fused to get an output imagery which is both spatially and spectrally of high resolution. This process of combining panchromatic and multispectral images is referred to as pansharpening. Pansharpening is a process of fusing a high spatial resolution panchromatic image with a high spectral resolution multispectral image to produce an image that is spatially and spectrally high in resolution. During the fusion process, the pansharpened output is often affected by the distortion of the spectral properties. It is of great importance that the spectral properties of the multispectral band are to be preserved in the pansharpened or fused image. To overcome this challenge, many researchers in the remote sensing field have devoted a lot of time to building a pansharpening method from different perspectives ranging from sensor-based models, machine learning, signal processing, super-resolution, neural networks, and so forth.

In the present study, IKONOS satellite image is used for illustration of the proposed method. The technical details of IKONOS data used in the study are provided in Appendix A.

Our objective is to provide a solution to the pansharpening problem using a data-centric approach aided by an information theoretic analysis. We consider pansharpening as the projection of panchromatic data onto spectral data using a classical result in information theory. The main contributions of the study can be summarized as providing a solution to the pansharpening problem based on orthogonal projection of panchromatic data onto the spectral band based on co-variance and cross-variance between pan and spectral data. To demonstrate the effectiveness of the proposed pansharpening method, we use a variety of evaluation criteria. The performance of the proposed method is also compared with that of many existing commonly used pansharpening methods using identical data.

The outline of the paper is as follows. Section 1 gives a brief introduction and a general idea about pansharpening. Section 2 surveys the literature related to the research work. Necessary background

information is provided in Section 3. Section 4 describes the proposed information theoretic approach to pansharpening. Section 5 provides experimental results based on the application of the proposed approach. A comparative study of the proposed method and the existing methods of pansharpening is carried out in Section 6. Lastly, the paper ends with a conclusion and future directions in Section 7.

2. RELATED WORKS

The remote sensing community has devoted a great deal of attention to overcoming the limitation of information obtained from a single source and providing a better understanding of the earth's observation surface. Many researchers have come forward with new ideas to develop fusion methods either by mitigating the effects of drawbacks of the existing or conventional image fusion methods or by building a fresh method from various perspectives. [1) proposed a pixel-level image fusion technique that is model-based and requires regularization of the pixel neighborhood to solve the satellite image fusion problem. [2] reported a fusion algorithm that integrates IHS and wavelet transform. The method uses IHS to preserve the spatial resolution and wavelet transform to preserve the spectral properties [3] proposed a fusion scheme that is based on the integration of curvelet transform and bi-dimensional empirical mode decomposition (BEMD). The proposed method is illustrated using IKONOS, QUICKBIRD, and GEOEYE satellite data and is compared with IHS, Brovey, PCA, and curvelet methods. [4] proposed a new fusion scheme by combining two different approaches namely Principal Component Analysis (PCA) and Non-Sub-sampled Contourlet Transform (NSCT). [5] proposed a pansharpening method based on linear regression. The proposed method is purely based on the reflectance data (pixel values) of the satellite imagery. As an extension to it, [6] proposed a data-centric pansharpening method based on optimization of a convex combination of spectral consistency and variance matching. Palsson et al. (2012) [7] applied various pansharpening techniques (such as IHS, Brovey, model based and multiresolution) to IKONOS and QUICKBIRD images and later used them for classification. The spatial information from the panchromatic data is derived using mathematical morphology. Helmy and El-tawel (3) proposed a fusion scheme which is based on the integration of curvelet transform and bi-dimensional empirical mode decomposition (BEMD). Curvelet transform is a very popular technique in image analysis that is used to represent image at different scales and different angles. BEMD is a two-dimensional extension of empirical mode decomposition (EMD) which is widely used for the decomposition of images into multiple components and residues to remove redundant data and extract the highest frequency components from the signal. Garzelli (2016) [8] did a review of pansharpening methods based on the super-resolution (SR) concept applied to image fusion framework. Super-resolution is the process of obtaining a high spatial resolution image from multiple low-resolution images. Chanussot et al. (2020) [9] proposed a benchmark comprising of 26 pansharpening methods which are tested on different scenarios. The methods belong to different classes ranging from classical methods to third generation approaches. In the thesis of Bidyarani (2020) [10], the researcher proposed three pansharpening methods namely spectral consistency, convex optimization and information theoretic approach. The researcher also performed a comparative study among the proposed three methods. Finally, it was concluded that the information theoretic approach outperforms the other methods as well taken into consideration. The performance of each of the method including the existing methods was assessed using standard evaluation metrics.

More recently, pansharpening methods have been proposed employing convolutional neural networks (CNN). The CNN methods are trained using domain data and tend to minimize the cost function involving the difference between the true data and the predicted one using a nonlinear mapping of the input data. In some cases, the residual between the true data and the interpolated value is also learnt. In CNN methods, the trained nonlinear functions involved tend to capture specific features of domain data which the algorithm or model-based methods cited above may miss. Hence, higher accuracy has

been reported using CNN methods. Two examples of CNN based pansharpening methods are cited below.

Masi et al. (2016) [11] proposed a pansharpening method from the deep learning perspective particularly. Unlike the artificial neural network, CNN can reduce the amount of connectivity among the neurons thereby reducing the number of learning parameters. He et al. (2019) [12] proposed a "detail injection-based convolutional neural network (DiCNN) pansharpening". The framework consists of two different techniques depending on the use of multispectral details and panchromatic images. Xi et al. (2022) [13] proposed an adaptive multistage pansharpening CNN known as AdapMSNet have shown superior performance in preserving the spatial details in the fused image. Jie Li et al. (2021) [14] proposed self-supervised learning method called CycleGAN which is based on cycle-conssitent generative adversarial network. The proposed method shows that it performs better than the existing unsupervised pansharpening method. Xingxing Li et al. (2023) [15] proposed a pansharpening method based on deep non-local unfolding. The method has shown the superiority of the proposed method compared to the state-of-the art methods.

3. INFORMATION THEORETIC RESULT

In this section, we describe briefly the information theoretic result of orthogonal projection of correlated data on which the proposed pansharpening method is based. The material presented follows closely the treatment given in [16]. Suppose x and y are two vectors in C^n with the inner product, denoted by <,> and defined as

$$<x,y> = xy^* \qquad (1)$$

where $x = [x^1, x^2 \ldots x^n]$, $y = [y^1, y^2 \ldots y^n]$ and $x^1, x^2 \ldots x^n$ represent scalar elements in x and $y^1, y^2, \ldots, y^n$ represent scalar elements in y. * represents conjugate transpose. The two vectors x and y are said to be orthogonal when their inner product is zero. That is <x, y> = 0. Consider a set of vectors $\{x_1, x_2, \ldots x_n\}$, $x_i \epsilon C^n$, $i=1, 2, \ldots n$ written in column form as x**= col {**$x_1, x_2, \ldots x_n$}.

The Gramian or Gram matrix, **G** of **x** is the matrix of all possible inner products of the vector elements of **x**. That is, G ($x_1, x_2, \ldots x_n$) = <**x, x>** = [<x_i, x_j >], i,j ε {1,2,3,..n}.

Let us now recall some basics from (16) as follows: It is assumed that $\{y_i\}$, y_i, ε C^n , i=0,1, 2,...N and $\{z_j\}$, z_j ε C^n, j=0,1,2, ...M, $M \leq N$, belonging to a Hilbert space H, are zero-mean random variables with their variance and cross-variances known. Let R_y denote the variance of $\boldsymbol{y}$ =col $\{y_o,..y_N\}$ and is given by the Gramian;

$$R_y = (\boldsymbol{y}, \boldsymbol{y}) \qquad (2)$$

Also, let R_{zy} denote the cross-variance of $\boldsymbol{z}$= col $\{z_o, \ldots, z_M\}$ and $\boldsymbol{y}$ and is given by the Gramian

$$Rzy = (\boldsymbol{z}, \boldsymbol{y}) \qquad (3)$$

Consider an arbitrary linear combination of $\{y_o,..y_N\}$, say $k^*\boldsymbol{y}$, where $k^* \in C^{(M+l)\times(N+l)}$ and $\boldsymbol{y}$ = col$\{y_o, \ldots, y_N\}$.

The inner product $\langle z_i, y_j \rangle = E(z_i y_j^*)$ where E(.) denotes expectation. Let P(k) be the mean-square-error (or error variance) matrix in estimating $\boldsymbol{z}$ using $k^*\boldsymbol{y}$, given by;

$$P(k) = E(z - k^*y)(z - k^*y)^* = || z - k^*y||_H^2 \quad (4)$$

where ||.||H corresponds to norm in the Hilbert space . The RHS of Eq. (4) is simply a generalization of the product of scalar and its conjugate to the outer product of a collection of vector elements and its conjugate.

The least-mean-square estimate which minimizes P(k) [16] is given by the projection of $\boldsymbol{z}$ on $H\{\boldsymbol{y}\}$, the Hilbert space spanned by the vector elements of $\boldsymbol{y}$, as follows

$$\hat{z} = k_o^*\boldsymbol{y},\ k_o^* \in C^{(M+1)x(N+1)} \quad (5)$$

where,

$$k_o^* = E(\boldsymbol{z}\boldsymbol{y}^*)\,[E(\boldsymbol{y}\boldsymbol{y}^*)]^{-1} = R_{zy}R_y^{-1} \quad (6)$$

This follows since

$$\begin{aligned} P(k) &= ||z - k^*y||_H^2 \\ &= ||z - \hat{z} + \hat{z} - k^*y||_H^2 \\ &= ||z - \hat{z}||_H^2 + ||\hat{z} - k^*y||_H^2 + ||< z - \hat{z}, \hat{z} - k^*y >||_H^2 \end{aligned} \quad (7)$$

Putting $k^* = k_o^*$ and applying (5), it follows that

$$P(k_0) = ||z - \hat{z}||_H^2 \quad (8)$$

Since the terms $||.||_H^2 \geq 0$ on the RHS of (7), it follows that $P(k) \geq P(k_0)$ with equality achieved only when $k = k_0$.

A simple orthogonal projection is shown in Figure. 1 can also be used to illustrate the above result.

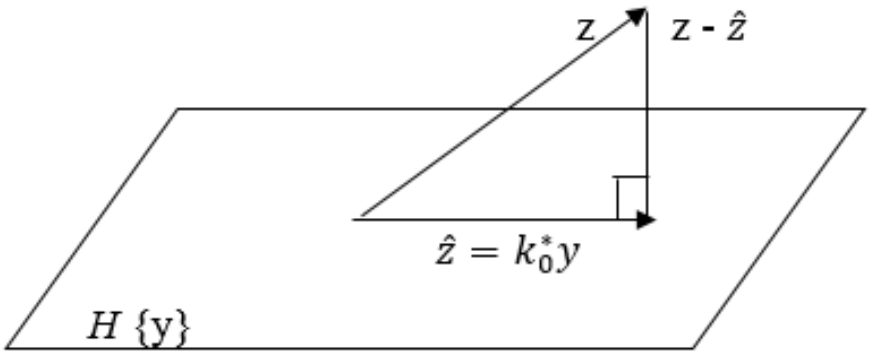

Figure 1. Projection of $\hat{z}=k_o^*\boldsymbol{y}$ in the Hilbert subspace

4. PROPOSED METHOD

Let us first consider the red band only. The other colors follow similarly. Let $z = [z_1, z_2, \ldots, z_8]$ be a 8-tuple data vector, z_i $i=1,2, \ldots, 8$, corresponding to the i^{th} column of *8×8 matrix* of red band data taken from left to right. The corresponding *32×32 panchromatic data* at the same location is down-sampled to *8×8 data*. The down-sampling has to be carried out as follows. Each *4× 4 panchromatic* data is to be averaged to *1×1 data* beginning from the left to right covering the *32× 32 panchromatic* data in 8 passes. This restriction on the method of down-sampling is to preserve the correlation between pan and spectral data. Let $y = [y_1, y_2, \ldots, y_8]$ correspond to a *8-tuple vector* so obtained.

Let y_i, $i=1,2, \ldots, 8$ correspond to the i-th column of the down-sampled panchromatic data. Let R_{zy} and R_y be determined using Eqs. (2) and (3) respectively. Determine the 8×8 matrix k_o^* as per Eq. (6)

$$k_o^* = R_{zy} R_y^{-1} \tag{9}$$

To complete the proposed pansharpening method, we proceed as follows. Considering the higher resolution (prior to down-sampling) 32×32 panchromatic data, use the k_o^* obtained in Eq. (6) repeatedly to each of 8× 8 data of panchromatic band beginning from left to right covering the 32×32 panchromatic data in four passes. The result in each step is a 8×8 data of the spectral band. Four passes left to right result in a 32×32 spectral band data. The complete pansharpening process is shown in Figure. 2.

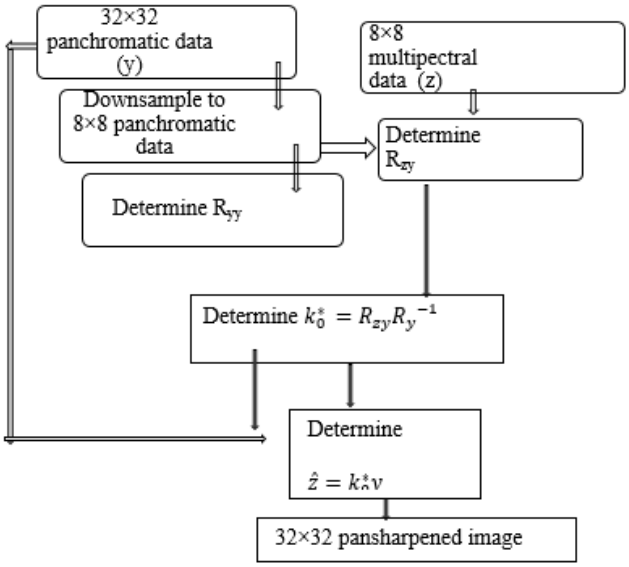

Figure 2. Pansharpening process based on information theoretic approach

5. EXPERIMENTAL RESULTS

The first step is to determine R_{zy} and R_{yy} using Eqs. (2) and (3) respectively and then find $\boldsymbol{k_o^*}$ using R_{zy} and R_{yy}. As stated, considering the higher resolution (prior to down-sampling) 32×32 panchromatic data (Figure. 3(a)), we down-sampleit to obtain the vector y = $[y_1, y_2, \ldots y_8]$ where y_i, i=1,2,...8 correspond to the i^{th} column of the down-sampled panchromatic 8×8 data. Considering the given 8×8 red band (Figure. 3(b)) as the 8-tuple vector z = $[z_1, z_2, \ldots z_8]$, z_i i=1,2,.8, being the i^{-th} column, R_{zy} and R_{yy} are obtained using Eqs. (1) and (2). $\boldsymbol{k_o^*}$ is then obtained as per Eq. (6). Repeatedly applying $\boldsymbol{k_o^*}$ to each of 8×8 data of panchromatic band (Figure. 3(a)) beginning from left to right covering the 32×32 panchromatic

data in four passes, results in 32×32 red band data as shown in Figure. 4(a). Similarly, the high-resolution green and blue bands are obtained as shown in Figure. 4(b) and 4(c) respectively. For validation of the computed data and comparison with the original 8×8 red data, the pansharpened 32×32 red data is down-sampled to 8×8 data points. The resulting 8×8 down-sampled pansharpened red, blue, and green are depicted in a monochromatic color in Figure. 5 (a), (b), and (c) for validation against ground truth data of Figure 3(b), (c), and (d) respectively.

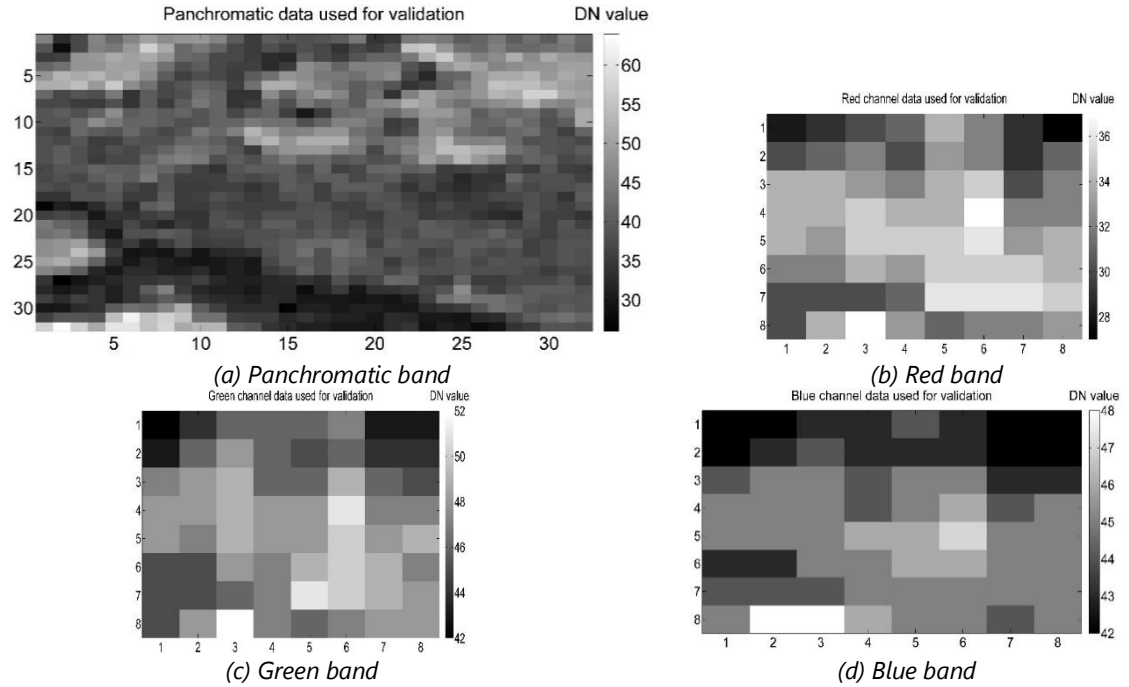

(a) Panchromatic band *(b) Red band*

(c) Green band *(d) Blue band*

Figure 3. (a) 32×32 Panchromatic pixel window and 8×8 Multispectral pixel window (b) red band (c) green band and (d) blue band.

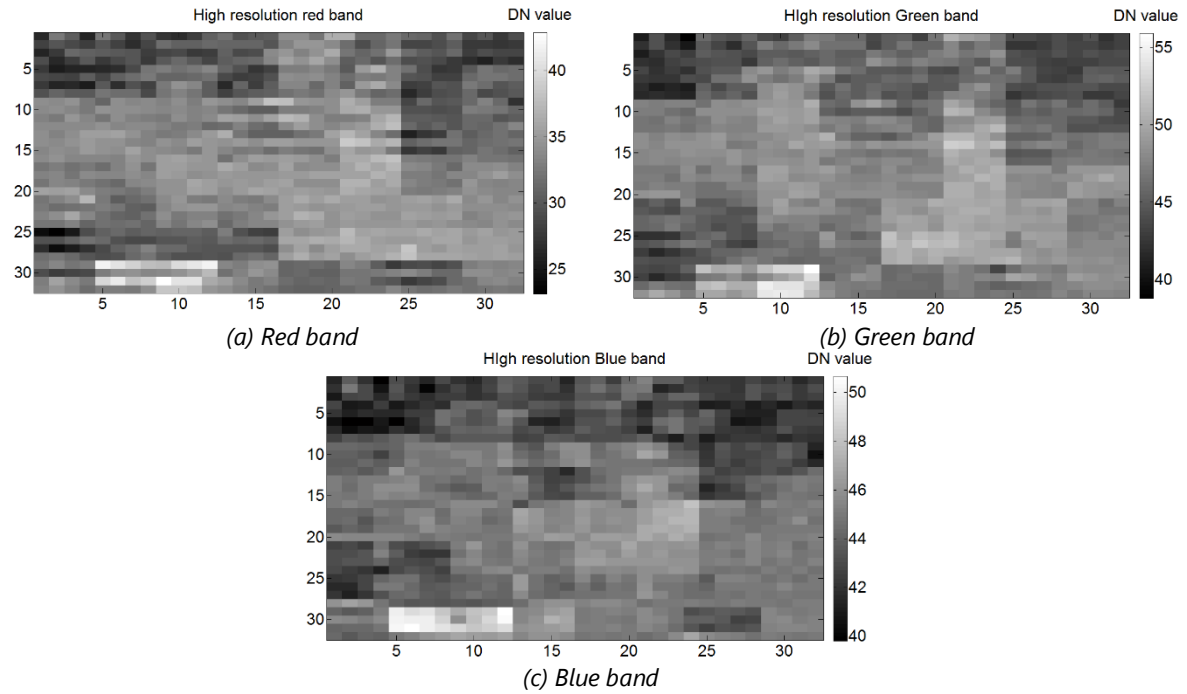

(a) Red band *(b) Green band*

(c) Blue band

Figure 4. Pansharpened high resolution multispectral data (a) red band (b) green band and (c) blue band.

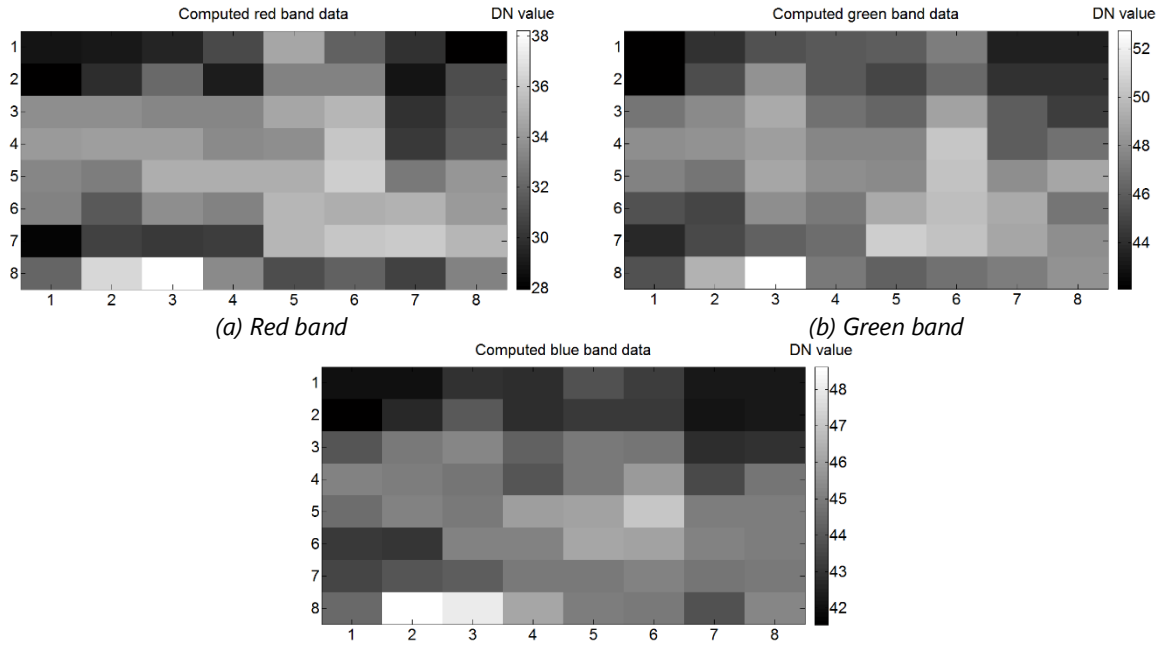

(a) Red band *(b) Green band*

(c) Blue band

Figure 5. Down-sampled pansharpened multispectral data for validation (a) red band (b) green band and (c) blue band.

6. PERFORMANCE COMPARISON

The fusion results obtained are assessed by the evaluation criteria discussed. Table 1 shows the performance of the proposed method against other methods. The evaluation of the result of all the pansharpening methods is done by comparing the pansharpened result with the ground truth of the respective dataset considered as a reference. For comparison of the proposed pansharpening method, the following existing methods are considered namely intensity hue saturation (IHS) [17, 18] Brovey [19], principal component analysis (PCA) [20], smoothing filter-based intensity modulation (SFIM) [21], high pass filter (HPF) [21] and Multiplication (Multi) methods [21]. The reason for choosing these existing methods for comparison is due to the fact that these methods are standard methods and analytical in nature. Similar to our proposed method, these existing methods are straightforward and can be applied to any image data. The existing methods are briefly described as follows.

6.1. Existing Method

In the IHS [17,18,22,23] pansharpening method, the RGB color space is transformed to IHS color space. The transformation can be performed using three bands only at a time. The step consists firstly of resampling the XS images to the spatial resolution of pan. Secondly, the transformation of resampled RGB to IHS color space is carried out. Thirdly, the intensity component is histogram matched with panchromatic band data. Fourthly, the intensity component is replaced by the histogram-matched panchromatic band data. Finally, the reverse transformation is applied to get the R, G, and B fused images.

The Brovey method [19], on the other hand, is a combination of pan and XS images. The method is based on image algebra involving multiplication and division operations. Each multispectral band is divided by the sum of all the bands and multiplied by pan. The output is given by,

$$F_{Brovey} = (X_i / R+G+B)\, Pan \qquad (10)$$

where X_i represents the i[th] multispectral band, i ε {R, G, B} for red, green and blue respectively. F_{Brovey} represents the fused output and Pan is the panchromatic image.

Smoothing filter-based intensity modulation (SFIM) (Yuan *et al.*, 2014) is a smoothing algorithm where a low pass filter is applied to a high-resolution pan channel. The low-resolution multispectral band is multiplied with the high-resolution pan band and is divided by the low pass filtered pan band. This is done for every band of the multispectral channel. The transformation is done as follows.

$$F_{SFIM} = \sum_j \sum_k \frac{M_{low_{i(j,k)}} \times P_{high_{(j,k)}}}{P_{lpf_{(j,k)}}},\ i = 1,2...n \qquad (11)$$

where F_{SFIM} represents the fusion output, i is the index representing the bands, $M_{low_{i(j,k)}}$ is the low-resolution multispectral band, $P_{high_{(j,k)}}$ is the high spatial resolution panchromatic band and $P_{lpf_{(j,k)}}$ represents the low pass filtered pan band. (j,k) represents the pixel location.

The high pass filter (HPF) [21] method involves high pass filtering of pan band with a window size of a 3×3 filter to extract the spatial content. The multispectral image is resampled to the same resolution as the panchromatic image. In this case, the multispectral band gets added with the high pass filtered pan band divided by 2. The fusion process can be mathematically presented as follows,

$$F_{HPF} = \sum_j \sum_k \frac{M_{low_{i(j,k)}} + P_{high_{(j,k)}}}{2},\ i = 1,2...n \qquad (12)$$

where F_{HPF} represents the fusion output, i is the index representing these bands, $M_{low_{i(j,k)}}$ is the low-resolution multispectral band and $P_{high_{(j,k)}}$ is the high spatial resolution panchromatic band that is filtered by a high pass filter. (j,k) represents the pixel location.

Principal component analysis (PCA) [20] is another commonly used method applied to image fusion which is based on statistical approach. It transforms a number of correlated variables into a number of uncorrelated variables. PCA based pansharpening involves resampling of the multispectral band to the resolution of the panchromatic band. First, the principal components (PC) are computed for each multispectral band, then the first PC is replaced with the histogram matched panchromatic band and finally an inverse PCA transformation is applied to get the fused output.

Multiplication (MULTI) transform [21] is another popular algorithm based on image algebra. This method is one of the simplest methods which consists of a simple multiplication. Each of the low-resolution multispectral band is multiplied with the high-resolution pan band with a corresponding weight.

$$F_{MULTI} = \sqrt{\sum_j \sum_k a.M_{low_{i(j,k)}} \times b.P_{high_{(j,k)}}},\ i = 1, 2...n \qquad (13)$$

where F_{MULTI} represents the fusion output, i is the index representing the bands, $M_{low_{i(j,k)}}$ is the low-resolution multispectral band and $P_{high_{(j,k)}}$ is the high spatial resolution panchromatic band. (j, k) represents the pixel location. The weights a and b are considered to be 1 each. The square root puts a limit on the brightness value avoiding very large values.

Identical datasets are used for comparison among all the fusion methods. Six evaluation metrics namely, Chi square ($\chi 2$) goodness of fit test, R^2 test, Root mean square error (RMSE), signal to noise ratio (SNR), spectral discrepancy (SD) and ERGAS are used to assess the performance of the fusion output of different methods. The performance of each of the methods will be assessed based on the numerical values

obtained through the evaluation metrics. Comparative analysis between the proposed method and the existing methods is performed based on these evaluation metrics. The implementation of each method is done using IKONOS sensor data as discussed in the earlier section.

6.2. Evaluation Metrics

6.2.1 Chi-square test ($\chi 2$)

Chi-square test (24) is a statistical tool that is helpful to evaluate the "goodness of fit" of the observed data and the expected data. The Chi square test ($\chi 2$) is given by the relation

$$\chi 2 = \Sigma (O_i - E_i)^2 / E_i \quad (14)$$

where O_i is the observed data that is used as the reference data, and E_i is the expected (i.e. computed) data.

6.2.2 R^2 Test

The R^2 test (also known as coefficient of determination) is a statistical tool widely used to test the correlation between two sets of data. R2 test is computed between the proposed methods and the IHS Brovey, PCA, SFIM, HPF and Multi methods. The R2 test is given as,

$$R^2 = 1 - (SSE/SSTO) \quad (15)$$

Where, SSTO = SSE + SSR, SSE and SSR are defined next. The sum of Error Squares (SSE): The sum of error squares is the condition for checking the spectral consistency between each point of the computed and the actual XS channels. SSE can be found as $SSE=\Sigma_i(y_i-\hat{y}_i)^2$ where y and $\hat{y}$ are the actual and computed values respectively and n is the number of observations in the sample. The sum of Regression squares (SSR): The SSR is calculated as $SSR=\Sigma_i(\hat{y}_i-\bar{y}_i)^2$ where $\hat{y}$ and $\bar{y}$ are the computed data and mean of the observed data respectively. The optimal value of R^2 is 1 indicating a strong correlation between the two data.

6.2.3 Root mean square error (RMSE)

Root mean square error (RMSE) [25] is defined as,

$$RMSE=\sqrt{\frac{\sum_{i=1}^{n}(\hat{x}_i-x_i)^2}{n}} \quad (16)$$

where x_i is the original multispectral data and $\hat{x}_i$ is the multispectral data. n corresponds to the number of data points in the sample.

6.2.4 Signal –to-noise-ratio (SNR)

The signal – to – noise - ratio (SNR) [26] can be calculated as follows;

$$SNR=\sqrt{\frac{\sum_{i=1}^{n}(\hat{x}_i)^2}{\sum_{i=1}^{n}(\hat{x}_i-x_i)^2}} \quad (17)$$

where x_i and $\hat{x}_i$ are the original and computed data respectively. n corresponds to the number of data points in the sample.

6.2.5 Spectral discrepancy (SD)

Spectral discrepancy [27] is usually done to check the spectral quality of the fusion result and is computed as follows,

$$SD=\frac{1}{N}\sum_{i=1}^{N}|\hat{x}_i - x_i| \quad (18)$$

6.2.6 ERGAS

ERGAS stands for "*Erreur Relative Globale Adimensionnelle de Synthesis*" in French. This metric is based on root mean square error (RMSE) and is used to calculate the amount of spectral distortion (28,29)

$$ERGAS=100\frac{h}{l}\sqrt{\frac{1}{Q}\sum_{q=1}^{Q}\left(\frac{RMSE\,(q)}{\mu(q)}\right)^2} \quad (19)$$

where (h/l) is the ratio of the pixels from pan to XS, $\mu(q)$ and q represent the mean of the q^{th} channel and the index of the band respectively and Q is the number of bands. For a good spectral quality, ERGAS value should be small.

Looking at the critical values in the Chi-squared ($\boldsymbol{\chi 2}$) goodness of fit test provided by each of the methods, the proposed method gives the least critical value thereby giving a significantly smaller p-value. Among the existing methods, the Multi-method gives a better fit than the rest with a better critical value and a smaller p-value. The inference that can be made from the critical value and p-value of the Chi-square goodness of fit can be briefly stated as follows. The smaller the critical value and the p-value, the better the fit of the data. The critical value indicates the degree of deviation of the computed data from the reference data. Therefore, a smaller critical value (CV) indicates less deviation and better spectral consistency. The p-value indicates the probability of getting a better fit than the one under evaluation. R^2 value involves both SSE and SSR. Since R^2 = 1 / {1+ (SSE/SSR)}, a smaller SSE /SSR ratio gives R^2 value close to the desirable unity. As can be seen in Table 1, the existing methods seem to result in a moderate R^2 value. This is because the SSR value obtained in these methods are very large (giving high variance compared to the actual) which gives a low SSE/SSR ratio even with a not-so-small SSE (that is, less spectral consistency). However, from all the methods considered the proposed method comes on top with high R^2 value very close to unity. From Table 1, the RMSE for the proposed method is found to result with the least values of 0.78, 0.42 and 0.20 respectively for red, green and blue band including the existing methods. Among the existing methods, Multi method provides the least RMSE value followed by the IHS. The SNR value gives the amount of information content in the fused output. As observed from Table 1, the signal to noise ratio (SNR) is the highest for the proposed approach with a value of 41.59, 109.7 and 218.5 for the red, green and blue bands respectively including the existing methods. A low value of spectral discrepancy indicates a good spectral quality. The spectral discrepancy is the lowest for the proposed method with values 0.55. 0.29 and 0.15 for red, green and blue band respectively. It is also observed that the proposed method gives the least ERGAS value.

7. CONCLUSION

Each pixel of the sensor image containing data on panchromatic band has necessary information on the spectral bands which constitute the panchromatic band. In a way, multispectral data can be assumed as a projection of pan data on to the spectral band in question. However, due to the difference in the

resolution of the pan and spectral data, pansharpening is more than a direct projection of pan data onto the spectral band. Fortunately, using the proposition that the correlation between the pan and the spectral data is inherent and is independent of the location of Earth's surface on which the satellite sensor is reflected, it follows that the correlation may be considered as independent of the resolution of the pan and spectral data. This is the line of reasoning which is taken in this study to proposed a pansharpening approach based on the result of orthogonal projection between two sets of correlated data drawn from information theory.

In this paper, we have formulated a proposal for pansharpening technique based on the reflectance data and using a classical result on orthogonal projection of correlated data from information theory. This approach is based on the cross variance and co-variance related to the pan and spectral channels. Based on the evaluation criteria discussed, the proposed method performs better than the other methods considered. This method of pansharpening can be extended to larger image data sets by fragmenting the larger data into smaller data sets and applying the proposed method repeatedly to cover the larger data set. The individual solutions can be integrated into a whole by applying a smoothing function at the boundaries.

As a future work, performance of a pansharpening method dependent on the distribution of source data can be considered. It will be useful to study the sensitivity of the performance indices of any pansharpening method to the extent of dispersion of the source data. Moreover, in view of the promise shown by the proposed information theoretic approach, the method could be extended to projection on to a Krein space (which is a generalization of Hilbert space considered in the paper) which could allow one to extract only the positively correlated spectral data from the panchromatic data. Finally, in future the residual data with respect to ground truth of the proposed method can also be tuned on the lines of convolutional neural network.

Table 1: Performance evaluation of proposed method and existing methods

Evaluation criteria	Multispectral Band	Theoretic approach	IHS	Brovey	PCA	SFIM	HPF	Multi
Critical value	Red	2.18	53.51	3142	789	55	911	27
	Green	1.27	34.43	4507	913	80	1361	36
	Blue	0.44	37.49	4249	1218	76	1277	21
p-value	Red	1.58E-33	0.56	1	1	0.25	1	2.01E-05
	Green	1.73E-40	0.03	1	1	0.92	1	0.0025
	Blue	2.39E-54	0.04	1	1	0.87	1	1.28E-07
R2test	Red	0.9	0.66	0.49	0.5	0.51	0.49	0.48
	Green	0.95	0.65	0.49	0.5	0.5	0.49	0.46
	Blue	0.97	0.6	0.49	0.5	0.51	0.49	0.44
RMSE	Red	0.78	4.79	22	27	6.29	15	3.96
	Green	0.42	4.79	32	34	9.11	22	4.88
	Blue	0.2	4.89	20	40	8.67	21	3.64
SNR	Red	41.59	6.59	0.46	2.2	5.82	1.1	9.07
	Green	109.7	8.79	0.47	2.38	5.77	1.07	8.82
	Blue	218.5	9.52	0.47	2.11	5.15	1.08	11.49
Spectral discrepancy	Red	0.55	4.02	1424	27.11	3.71	15.52	3.12
	Green	0.29	4.05	2047	33.99	5.38	22.67	4.31
	Blue	0.15	4.12	1932	40.01	5.12	21.35	3.09
ERGAS		0.29	5.04	29.59	35.43	8.39	20.84	4.35

REFERENCES

[1] Aanaes H, Sveinsson JR, Nielsen AA, Bovith T, Benediktsson JA. Model-Based Satellite Image Fusion. *IEEE Trans Geosci Remote Sens. 2008*; 46(5): 1336–46.

[2] Hong G, Zhang Y, Mercer B. A Wavelet and IHS Integration Method to Fuse High-Resolution SAR with Moderate Resolution Multispectral Images. *Photogramm Eng Remote Sens. 2009*; 75(10): 1213–23.

[3] Helmy AK, El-tawel GS. An integrated scheme to improve pan-sharpening visual quality of satellite images. *Egypt Informatics J. 2015*; 121–31.
[4] Ourabia S, Boumediene TH, Smara Y. A new Pansharpening Approach Based on NonSubsampled Contourlet Transform Using Enhanced PCA Applied to SPOT and ALSAT-2A Satellite. *J Indian Soc Remote Sens. 2016*; 44(February) :665–674.
[5] Devi MB, Devanathan R. Pansharpening using data-driven model based on linear regression. 2018 IEEE *Int Conf Electron Comput Commun Technol CONECCT 2018*. 2018; 1–5.
[6] Bidyarani Devi M, Devanathan R. Pansharpening using data-centric optimization approach. *Int J Remote Sens. 2019*; 40(20): 7784–804. DOI: https://doi.org/10.1080/01431161.2019.1602794
[7] Pálsson F, Sveinsson JR, Member S, Benediktsson JA. Classification of Pansharpened Urban Satellite Images. *IEEE J Sel Top Appl Earth Obs Remote Sens. 2012*;5(1): 281–97.
[8] Garzelli A. A review of image fusion algorithms based on the super-resolution paradigm. *Remote Sens. 2016*;8(10):1.
[9] Addesso P, Vivone G, Restaino R, Chanussot J. A Data-Driven Model-Based Regression Applied to Panchromatic Sharpening. *IEEE Trans Image Process. 2020*;29:7779–94.
[10] Devi MB. Pansharpening With Panchromatic And Multispectral Remote Sensing Data. *Hindustan Institute Of Technology And Science;* 2020.
[11] Masi G, Cozzolino D, Verdoliva L, Scarpa G. Pansharpening by convolutional neural networks. *Remote Sens. 2016*; 8(7).
[12] He L, Rao Y, Li J, Chanussot J, Plaza A, Zhu J. Pansharpening via Detail Injection Based Convolutional Neural Networks. *IEEE J Sel Top Appl Earth Obs Remote Sens. 2019*;
[13] Xie J, He L. Two-Stage Fusion based CNN for Hyperspectral Pansharpening. In: *IGARSS 2022 - 2022 IEEE International Geoscience and Remote Sensing Symposium. 2022*. p. 1091–4.
[14] Li J, Sun W, Jiang M, Yuan Q. Self-Supervised Pansharpening Based on a Cycle-Consistent Generative Adversarial Network. *IEEE Geosci Remote Sens Lett. 2022*;19:1–5.
[15] Li X, Li Y, Shi G, Zhang L, Li W, Lei D. Pansharpening Method Based on Deep Nonlocal Unfolding. *IEEE Trans Geosci Remote Sens. 2023*; 61: 1–11.
[16] Hassibi B, Sayed AH, Kailath T. Linear estimation in Krein spaces-Part I: Theory. *IEEE Trans Automat Contr. 1996*; 41(1): 18–33.
[17] Carper WJ, Lillesand TM, Kiefer RW. The use of intensity-hue-saturation transformations for merging SPOT panchromatic and multispectral image data. *Photogramm Eng Remote Sens. 1990*; 56(4): 459–67.
[18] Tu TM, Huang PS, Hung CL, Chang CP. A fast intensity-hue-saturation fusion technique with spectral adjustment for IKONOS imagery. *IEEE Geosci Remote Sens Lett. 2004*; 1(4): 309–12.
[19] Gillespie AR, Kahle AB, Walker RE. Color enhancement of highly correlated images. II. Channel ratio and "chromaticity" transformation techniques. *Remote Sens Environ [Internet]. 1987*, 22(3): 343–65.
[20] Pat S. Chavez, Jr. SCS and JA. Comparison of Three Different Methods to Merge Multiresolution and Multispectral Data: *LANDSAT TM and SPOT Panchromatic: 1991*; 57(3): 295–303.
[21] Yuan D, Hong X, Yu S, Li L, Zhao Y. Analysis of four remote image fusion algorithms for landsat7 ETM+ PAN and multi-spectral imagery. *Int J Online Eng. 2014*; 10(3): 49–52.
[22] Chavaz P., Jr. and Bowell J.A. Comparison of the spectral information content of Landsat thematic mapper and SPOT for three different sites in the Phoenix, Arizona region. *Photogramm Eng Remote Sensing. 1988*; 54(12)
[23] Edwards K, Davls PA. The Use of Intensity-Hue-Saturation Transformation for Producing Color-Shaded Relief Images. *Photogramm Eng Remote Sens. 1994*; 60: 1369–74.
[24] Plackett RL. Karl Pearson and the Chi-Squared Test. *Int Stat Rev / Rev Int Stat. 1983*.
[25] Aleksandra Grochala and Michal K. Satellite Imagery Data Fusion. *Remote Sens. 2017*; (9): 11–3.
[26] Yuhendra, Alimuddin I, Sumantyo JTS, Kuze H. Assessment of pan-sharpening methods applied to image fusion of remotely sensed multi-band data. *Int J Appl Earth Obs Geoinf [Internet]. 2012* Aug;18: 165–75.
[27] Yakhdani MF, Azizi A. Quality assessment of image fusion techniques for multisensor high-resolution satellite images *(CASE STUDY: IRS-P5 AND IRS-P6. 2010*; 38: 204–9.
[28] Alparone L, Wald L, Chanussot J, Thomas C, Gamba P, Bruce LM. Comparison of pansharpening algorithms: Outcome of the 2006 GRS-S data-fusion contest. *IEEE Trans Geosci Remote Sens. 2007*; 45(10): 3012–21.
[29] Du Q, Younan NH, King R, Shah VP. On the performance evaluation of pan-sharpening techniques. *IEEE Geosci Remote Sens Let. 2007*; 4(4): 518–22.

Appendix A

Ikonos Data00 Details

This appendix provides the IKONOS data used in the present work for carrying out the experimental work. Figure A 8.1 shows the full image captured by the IKONOS sensor. The size of the image is 22492×21176 pixels for panchromatic image and 5623×5294 pixels for multispectral image. A smaller part of the whole image has been used in the study for illustration of the fusion results.

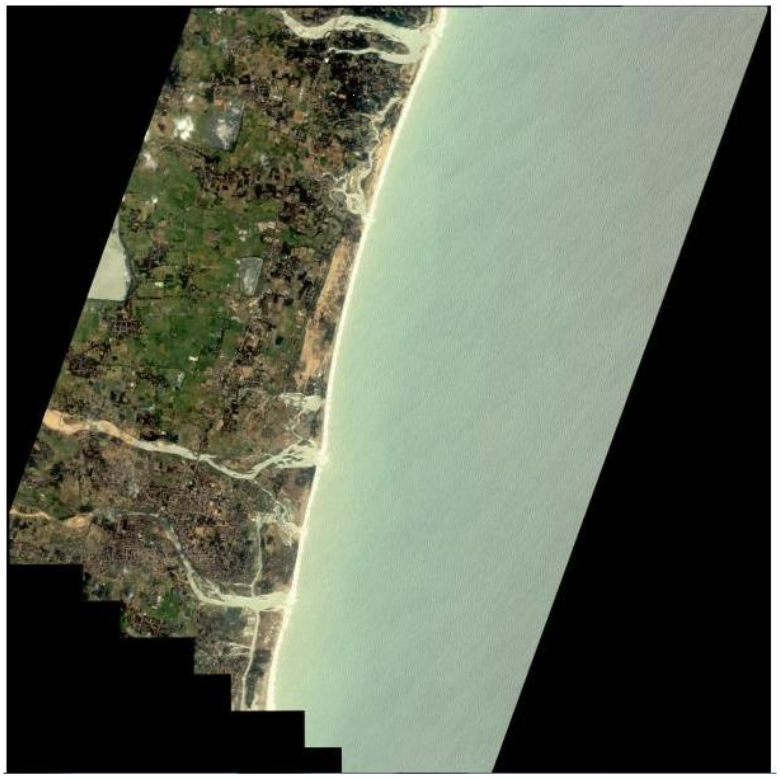

Figure 6. IKONOS Image

Table 2. IKONOS image details

Entity ID	IK220041229052900M00
Acquisition Date	2004/12/29
Cloud cover	0
Vendor	Space Imaging/GeoEye
Satellite	IKONOS-2
Sensor	MSI
Number of bands	5
Map projection	UTM
UTM Zone	44N
Datum	WGS84
Processing Level	GEOMETRICALLY CORRECTED
File Format	GEOTIFF
Pixel Size X	1.00000
Pixel Size Y	1.00000